Inverse offset method for adaptive cutter path generation from point-based surface

Prasenjit Kayal[a, b]

[a]School of Engineering (Mechanical), University of Birmingham, Edgbaston, Birmingham B15 2TT, UK

[b]Present address: Engineering and Technology Development, Engineers India Limited, 1, Bhikaiji Cama Place, New Delhi 110066, India

Email: p.kayal@eil.co.in

Abstract

The inverse offset method (IOM) is widely used for generating cutter paths from the point-based surface where the surface is characterised by a set of surface points rather than parametric polynomial surface equations. In the IOM, cutter path planning is carried out by specifying the grid sizes, called the step-forward and step-interval distances respectively in the forward and transverse cutting directions. The step-forward distance causes the chordal deviation and the step-forward distance produces the cusp. The chordal deviation and cusp are also functions of local surface slopes and curvatures. As the slopes and curvatures vary over the surface, different step-forward and step-interval distances are appropriate in different areas for obtaining the machined surface accurately and efficiently. In this paper, the chordal deviation and cusp height are calculated in consideration with the surface slopes and curvatures, and their combined effect is used to estimate the machined surface error. An adaptive grid generation algorithm is proposed, which enables the IOM to generate cutter paths adaptively using different step-forward and step-interval distances in different regions rather than constant step-forward and step-interval distances for entire surface.

Key Words: Inverse offset method, point-based surface, machined surface error, adaptive cutter path generation

1. Introduction

Sculptured surfaces are widely used in the aerospace, automobile, shipbuilding and die/mould manufacturing industries. These surfaces are usually finished by a 3-axis computer numerically controlled (CNC) milling with a ball-end mill. Milling is the process of material removal due to the interaction of a cutting tool moving relative to the workpiece. The desired surface is obtained as the tool comes in contact

with the workpiece along specific trajectories called cutter paths. Generating accurate cutter paths in an efficient manner is very important in many manufacturing industries [1]. The accuracy and efficiency of CNC machining is dependent on the cutter path planning which is a fundamental task in CNC machining [2]. The techniques of cutter path planning based on the path topology are generally classified: iso-parametric, iso-plane and iso-scallop [3].

In iso-parametric method, the cutter contact (CC) points are generated by increasing uniformly the parametric value of the part surface, and the cutter location (CL) point is calculated using the cutter radius and surface normal vector at every CC-point. In 1987, Loney and Ozsoy [4] proposed iso-parametric method, which was further improved as an adaptive method by Elber and Cohen [5]. The iso-parametric cutter paths are often much denser in one surface region than the others due to the non-uniform transformation between the parametric and Euclidean space, which results in varying cusp height distribution on the machined surface, and inefficient machining [6], and often have gaps, overlaps and loops which cause overcutting (gouging) [7].

In iso-plane method, cutter paths are computed by intersecting the part surface with a series of planes. This method is characterized with a uniform interval between adjacent cutter paths in the Euclidean space. If the slicing plane is parallel to the xy-plane, it is called the constant-z cutter path [8], and if the slicing plane is vertical, it is called the raster cutter path [3]. Although iso-planar tool path is very much popular and widely used in surface machining due to its robustness and simplicity, the cusp height increases sharply when the slope of the part surface is large. To limit the cusp height, the interval of the slicing planes is to be changed or new slicing planes are inserted in the region with a large scallop. The strategy is to decompose the surface into different regions according to different ranges of the surface slopes. The concept of iso-photes is used for the surface decomposition in [9].

In iso-scallop method, the path interval is determined such that the scallop height is being kept constant. A master CC-path is selected on the surface and for each point on the master CC-path, the next CC-path point is computed by offsetting the current path by the amount of computed CC-path interval to satisfy the scallop height. Constant scallop height tool path generation has been reported by Suresh and Yang [10] and Lin and Koren [11]. Given a cutter path, the iso-scallop curve is generated by Feng and Li [6] using the bisecting search method, which is replaced by Newton iterative algorithm in [12] to reduce the computation time. Redundant machining in iso-parametric and iso-planar methods is minimized since the scallop height is constant. Although the overall cutter path length is reduced significantly compared to other two methods, it suffers due to inexact determination of curvature in the cutter path direction and problem of conversion from Cartesian domain to parametric domain [2]. However, all these cutter path planning techniques focus on the surfaces defined by explicit/implicit surface equations.

Recently, the sculptured surfaces are characterised by a set of points lying on the surface, which is defined as the point-based surface and the cutter paths are generated directly from the point data [13]. Several approaches have been proposed to generate cutter paths from the point data. Lin and

Liu [14] suggest methods to generate rough and finish tool paths directly from large set of surface points lying in parallel planes. They construct a z-map model where the part surface height at each z-map point is calculated by linear interpolation from the measured points. Park and Chung [15] generate cutter paths form point sequence curves which are generated by linearly connecting the point data. To generate cutter paths from 3D regular/irregular point data, Kishinami *et al.* [16] propose the inverse offset method (IOM) that is derived based on the concept of machining a single point in space using an arbitrarily shaped tool. As the IOM has a number of desirable properties which make it particularly well suited for generating cutter paths from the point-based surface [13, 17]. The major beneficial feature of the IOM is that it generates self-interference free planar/non-planar cutter paths in a simple manner. In the IOM, the cutter paths are planned on the xy-plane by generating the grid sizes called the step-forward and step-interval distances respectively in the forward and transverse cutting directions. Several authors [7, 13, 14, 18, 19] have generated cutter paths using the IOM with constant grid sizes. Among them, Lin and Liu [14] have proposed insertion of additional CL-points in tangent discontinuous regions in order to reduce the machined surface error.

The local gouging is essentially a chordal deviation which is dependent on the step-forward distance and the cusp is dependent on the step-interval distance. The chordal deviation and cusp are also functions of the local surface slopes and curvatures. As the slopes and curvatures vary over the surface, different grid sizes are appropriate in different areas for obtaining the machined surface within tolerance [9, 20]. If the entire surface is machined with the smallest grid sizes in the forward and transverse directions, there will be redundant CL-point data in some regions and the machining efficiency will be reduced drastically. Therefore, it is critical to recognize the geometric features of the point-based surface within cutter path planning in order to achieve the machined surface with the desired accuracy, and with considerable reduction of the machining time [21, 22]. The aim of this paper is to generate cutter paths from the point-based surface using the IOM with the adaptive grid sizes determined based on the surface slopes and curvatures rather than constant grid sizes so that the machined surface error due to the chordal deviation and cusp can be limited within tolerance.

This paper is organised as follows. The cutter path generation from the point-based surface using the IOM is described in section 2. The error analysis due to cutter path planning is provided in section 3, and an algorithm for adaptive cutter path planning is proposed in section 4. A machining example is presented in section 5 to demonstrate the effectiveness of the algorithm, and final conclusion is provided in section 6.

2. Cutter path generation

In the point-based approach, the shape of a surface is characterised by a set of surface points rather than explicit/implicit surface equations [12]. The sets of points can easily be obtained for curvature continuous parts and coordinate measuring machines or laser scanners can sample the point data in reverse engineering applications. These points characterise an equivalence class of surfaces which are the same shape within tolerance. The density of the surface points is dictated by the required tolerance of the characterised surface. Given an initial grid of data, an interpolatory subdivision scheme inserts extra data points between the existing points so that denser set of surface points is generated for generating cutter paths with the desired accuracy [13].

The dense set of points which ensure the accuracy of generated cutter paths within tolerance is considered for the IOM operation. In the IOM, a 2D grid of points is prepared in the xy-plane using constant grid sizes g^x and g^y respectively in the x and y directions, as shown in figure 1(a) where x is the forward direction and y is the transverse direction. Then the cutter centre point of the inverted tool is placed at each surface point. Through each grid point in the cutter contact (CC)-region (tool shadow area), a line running parallel to the tool axis is constructed. These grid lines intersect with each inverted tool. The highest intersection point (z-height) is considered as the valid CL-point for each grid line and others are invalid CL-points, which are shown in figure 1(a). The raster tool path strategy is shown in figure 1(b). Various finish machining strategies including raster, radial, spiral, constant-z and 3D-offset are available [23-25]. The work presented in the paper is applicable to all finish strategies; however, the grid generation method and the error analysis are carried out only for the raster strategy.

The slopes and curvatures can be determined from the offset surface generated by the IOM with constant grid sizes g^x and g^y in the x and y directions respectively. The IOM-based cutter paths produce the chordal deviation in the xz-plane and the cusp height in the yz-plane. In order to calculate the precise value of the chordal deviation and cusp height, the slopes and curvatures are calculated from the initial offset surface. Figure 1(c) shows a rectangular area bounded by $\mathbf{CL}_{i,j}$, $\mathbf{CL}_{i+1,j}$, $\mathbf{CL}_{i+1,j+1}$ and $\mathbf{CL}_{i,j+1}$ which is called the bounded area throughout the paper. Given a rectangular grid of CL-points, the slope angles $\alpha_{i,j}^x$ and $\alpha_{i,j}^y$ respectively in the x and y directions for the bounded area are computed as follows:

$$\alpha_{i,j}^x = \cos^{-1} \frac{g^x}{\left\| \mathbf{CL}_{i,j}\mathbf{CL}_{i+1,j} \right\|} \tag{1}$$

$$\alpha_{i,j}^y = \cos^{-1} \frac{g^y}{\left\| \mathbf{CL}_{i,j}\mathbf{CL}_{i,j+1} \right\|} \tag{2}$$

The radii of curvature $\rho_{i,j}^x$ and $\rho_{i,j}^y$ in the x and y directions at every CL-point are estimated using a circle-based five-point formula of Tookey and Ball [26] except at the first two and last two points of every string of points, where a three-point formula is used. The radius of curvature is considered positive if the curve is locally convex, and negative if it is concave. It is also assumed that the curvature variations over a bounded area are limited by the curvatures at the four corner points. The slopes and curvatures are used to the error analysis for cutter path planning in the following section.
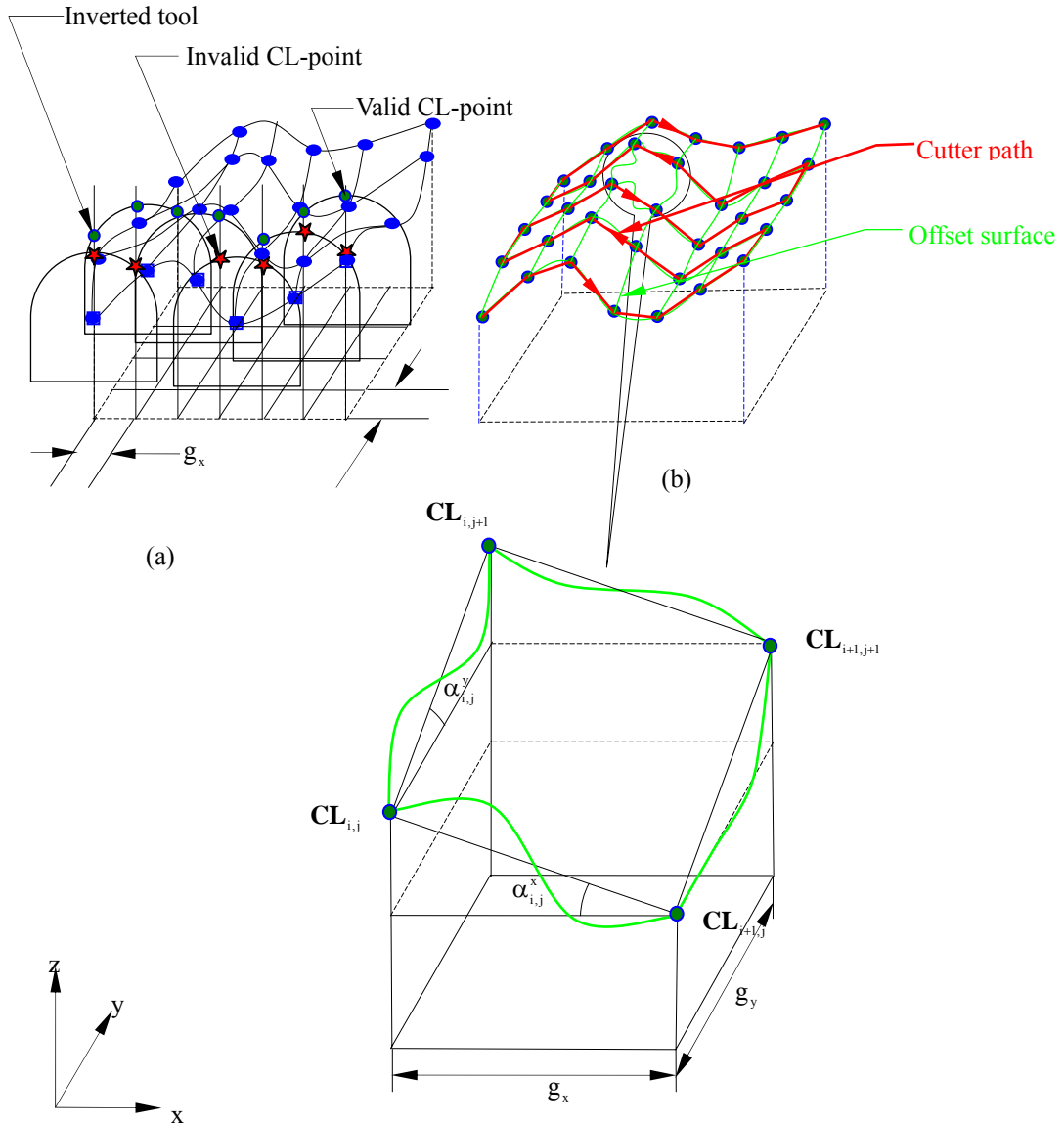

Fig. 1. Cutter path generation: (a) IOM operation (b) Offset surface
and (c) Slope angles for CL-segments

3.   Error analysis for cutter path planning

In order to machine a part surface, one needs to consider the cutting effect on the machined

surface while the tool moves along a specified cutter path. The chordal deviation due to the step-forward distance and the cusp height due to the step-interval distance are evaluated respectively in sub-sections 3.1 and 3.2. The machined surface error is estimated as combined effect of the chordal deviation and cusp height in sub-section 3.3.

3.1 Chordal deviation

When the cutter path is approximated by connecting adjacent CL-points by straight line segments, the contour error is the deviation of the path from the corresponding CL-curve. This error is defined as the chordal deviation. In this sub-section, given a step-forward distance $(g_x > 0)$, the mathematical formula for the chordal deviation is derived in terms of the slope and curvature of the CL-curve segment in the forward direction.

Figure 2 shows two adjacent points $\mathbf{CL}_{i,j}$ and $\mathbf{CL}_{i+1,j}$ on a CL-curve in the xz-plane. Assuming that the CL-curve segment, in general, is a combination of positive and negative deviation, as shown in figure 2, the upper bound of the chordal deviation is calculated by approximating the CL curve segment with a circular arc. As the radius of curvature at any point on the CL-curve segment is bounded by the radii of curvature at the two end points, the radius of the circular arc is considered as a linear combination of the radii of curvature at the two end points. Figure 2 shows that the circular arc of radius $\rho_1 = \beta\rho_{i,j}^x + (1-\beta)\rho_{i+1,j}^x$ where $0 \le \beta \le 1$, is centred at O. The effect of β on the chordal deviation will be investigated later in this sub-section. The point $\mathbf{CL}_{m,j}$ is constructed on the circular arc so that the unit tangent vector at $\mathbf{CL}_{m,j}$ is parallel to the chord vector $\mathbf{CL}_{i,j}\mathbf{CL}_{i,j+1}$.
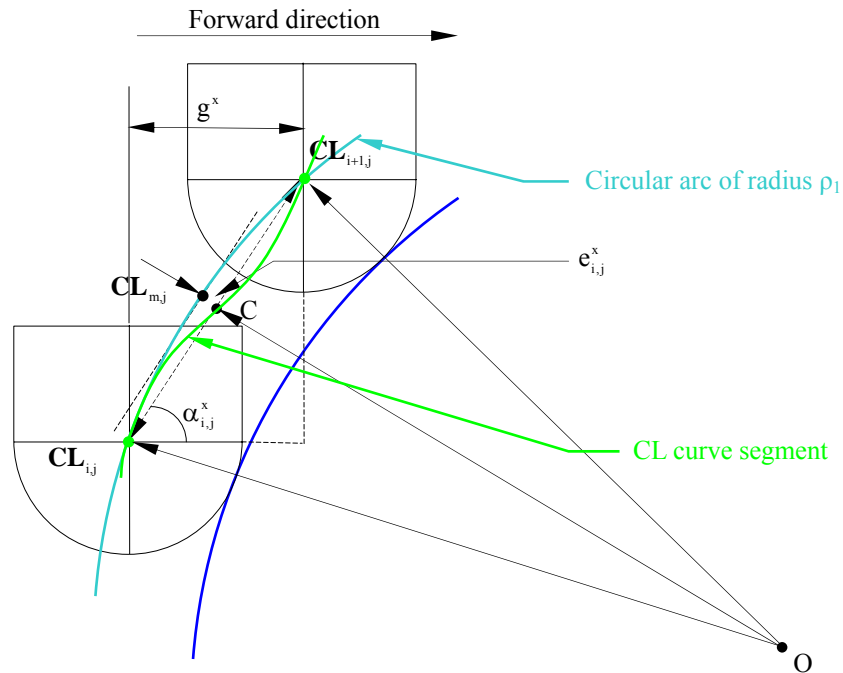

Fig. 2. Chordal deviation in forward direction

The cutting error at $\mathbf{CL}_{m,j}$ for $\rho_1 > 0$ is given by:

$$e_{i,j}^x = \rho_1 - \sqrt{\rho_1^2 - \left(\frac{\|\mathbf{CL}_{i,j}\mathbf{CL}_{i+1,j}\|}{2}\right)^2} \qquad (3)$$

The chord length $\|\mathbf{CL}_{i,j}\mathbf{CL}_{i+1,j}\|$ is related to the grid size g^x by:

$$\|\mathbf{CL}_{i,j}\mathbf{CL}_{i+1,j}\| = \frac{g^x}{\cos\alpha_{i,j}^x} \qquad (4)$$

Substituting Eq.(4) into Eq.(3), the chordal deviation for $\rho_1 > 0$ is given by:

$$e_{i,j}^x = \rho_1 - \sqrt{\rho_1^2 - \left(\frac{g^x}{2\cos\alpha_{i,j}^x}\right)^2} \qquad (5a)$$

Similarly, the chordal deviation for $\rho_1 < 0$ is given by:

$$e_{i,j}^x = \rho_1 + \sqrt{\rho_1^2 - \left(\frac{g^x}{2\cos\alpha_{i,j}^x}\right)^2} \qquad (5b)$$

Substituting $\rho_1 = \beta\rho_{i,j}^x + (1-\beta)\rho_{i+1,j}^x$ into Eq. (5), it could be proved that $e_{i,j}^x(\beta)$, a non-constant function of β for variable radii of curvature at the two end points, does not have any maxima or minima. Therefore, $e_{i,j}^x(\beta)$ is either monotonically decreasing or increasing function of β and the extreme values of $e_{i,j}^x(\beta)$ lie only at $\beta = 0$ and $\beta = 1$ for definite interval of $0 \leq \beta \leq 1$. Assuming that the radii of curvature, in general, are different at the two end points, $\max(e_{i,j}^x)$ and $\min(e_{i,j}^x)$ are determined by substituting the radii of curvature $\rho_{i,j}^x$ at $\mathbf{CL}_{i,j}$ and $\rho_{i+1,j}^x$ at $\mathbf{CL}_{i+1,j}$ for ρ_1 in Eq. (5).

3.2 Cusp height

The region left unmachined between consecutive cutter paths in the transverse direction is called the scallop or cusp [10]. The upper limit on the height of the cusp is called the cusp height. In this section, given a step-interval distance $(g^y > 0)$ and cutter radius R, the mathematical formula of the cusp height is derived in terms of the slope and curvature of the CL-curve segment in the transverse direction. Figure 3 shows the two points $\mathbf{CL}_{i,j}$ and $\mathbf{CL}_{i,j+1}$ on adjacent CL-curves in the yz-plane and the corresponding CC-points are $\mathbf{CC}_{i,j}$ and $\mathbf{CC}_{i,j+1}$. Like the CL curve segment in the forward direction presented in sub-section 3.1, the CL-curve segment $\mathbf{CL}_{i,j}\mathbf{CL}_{i,j+1}$ in the transverse direction is also approximated by a circular arc with a radius $\rho_2 = \beta\rho_{i,j}^y + (1-\beta)\rho_{i,j+1}^y$ where $0 \leq \beta \leq 1$, as a linear combination of the radii of

curvature at the two end points. The underlying assumption is that the surface is machinable with a ball-end mill of radius R. The cusp height [10, 11] for $\rho_2 > 0$ is given by:

$$e_{i,j}^y = \sqrt{\rho_2^2 - \left(\frac{\rho_2 \left\| \mathbf{CC}_{i,j} \mathbf{CC}_{i,j+1} \right\|}{2(\rho_2 - R)}\right)^2} - \sqrt{R^2 - \left(\frac{\rho_2 \left\| \mathbf{CC}_{i,j} \mathbf{CC}_{i,j+1} \right\|}{2(\rho_2 - R)}\right)^2} - (\rho_2 - R) \tag{6}$$

The relationship between the chord length $\left\| \mathbf{CC}_{i,j} \mathbf{CC}_{i,j+1} \right\|$ and grid size g^y is given by:

$$\left\| \mathbf{CC}_{i,j} \mathbf{CC}_{i,j+1} \right\| = \frac{g^y}{\cos \alpha_{i,j}^y} \left(\frac{\rho_2 - R}{\rho_2}\right) \tag{7}$$
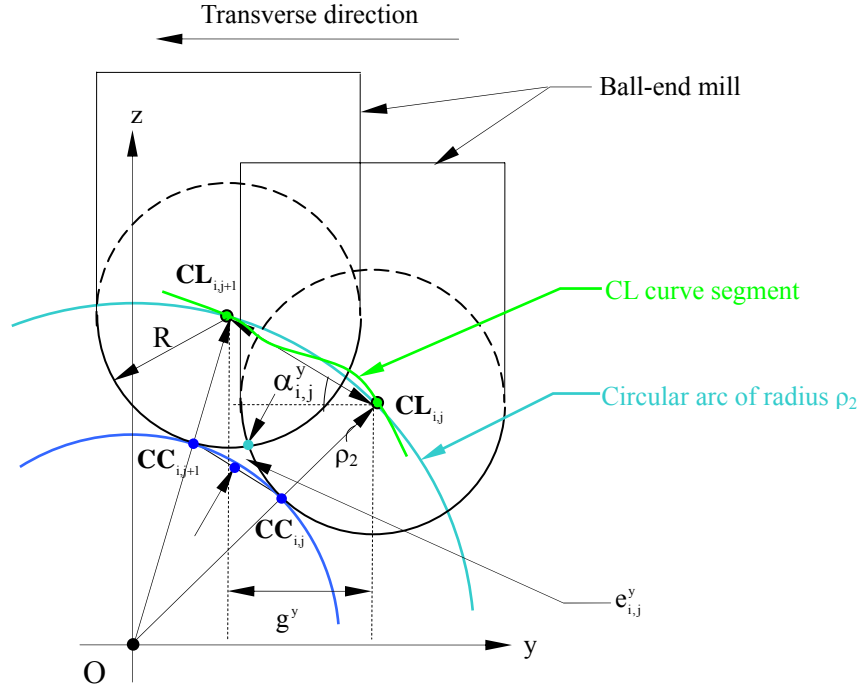

Fig. 3. Cusp height in transverse direction

Substituting Eq. (7) into Eq. (6), the cusp height for $\rho_2 > 0$ is given by:

$$e_{i,j}^y = \sqrt{\rho_2^2 - \left(\frac{g^y}{2 \cos \alpha_{i,j}^y}\right)^2} - \sqrt{R^2 - \left(\frac{g^y}{2 \cos \alpha_{i,j}^y}\right)^2} - (\rho_2 - R) \tag{8a}$$

Similarly, the cusp height for $\rho_2 < 0$ is given by:

$$e_{i,j}^{y} = \sqrt{\rho_2^2 - \left(\frac{g^y}{2\cos\alpha_{i,j}^y}\right)^2} + \sqrt{R^2 - \left(\frac{g^y}{2\cos\alpha_{i,j}^y}\right)^2} + (\rho_2 - R) \tag{8b}$$

It is noted that the Eq. (8b) always gives the negative cusp height for $\rho_2 < 0$. As the cusp height is the excess material over the machined surface, the absolute value is considered for the error evaluation. Like the chordal deviation, $e_{i,j}^y(\beta)$ is also either monotonically decreasing or increasing function of β and the extrema of $e_{i,j}^y(\beta)$ lie only at $\beta = 0$ and $\beta = 1$ for the definite interval of $0 \le \beta \le 1$. Assuming that the radii of curvature, in general, are different at the two end points, the upper bound of the cusp height $\max(e_{i,j}^y)$ is determined by substituting the radii of curvature $\rho_{i,j}^y$ at $\mathbf{CL}_{i,j}$ and $\rho_{i,j+1}^y$ at $\mathbf{CL}_{i,j+1}$ for ρ_2 in Eq. (8).
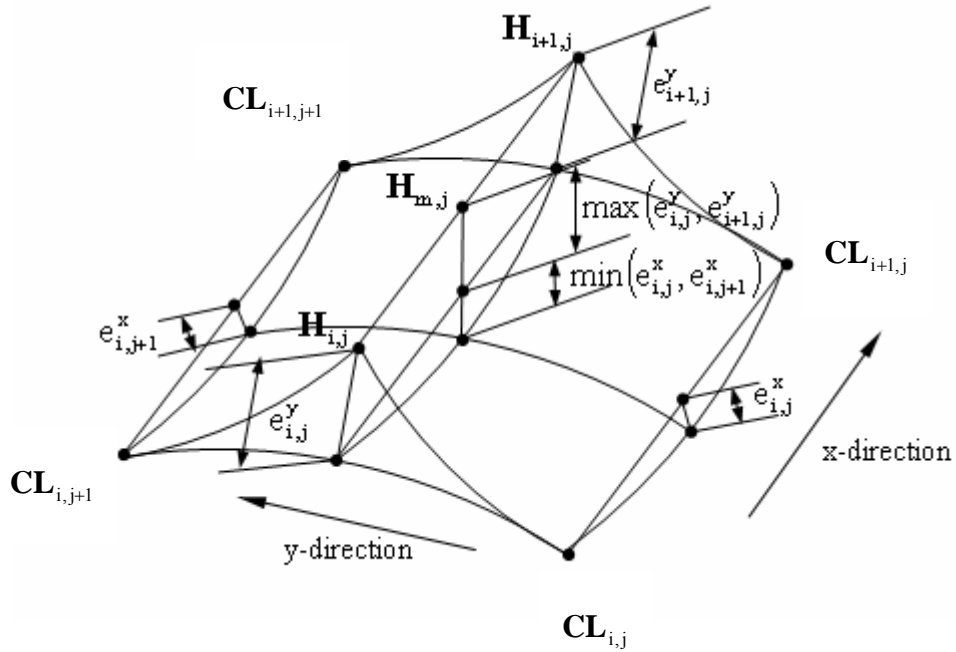

Fig. 4. Combined error at intermediate point

3.3 Machined surface error

The error due to cutter path planning presented in this sub-section is defined as the machined surface error and the presence of other sources of error generally exaggerates its estimation. The machined surface error is, notionally, a combined effect of the chordal deviation and cusp height [27]. For the bounded area, the maximum error is usually within the bounds determined for the boundary segments. The only configuration in which it is necessary to consider the combined effect $e_{i,j}^c$ is when $\min(e_{i,j}^x, e_{i,j+1}^x) < 0$, as illustrated in figure 4. Then the resultant machined surface error is given by:

$$e_{i,j}^c = \max\left(e_{i,j}^y, e_{i+1,j}^y\right) - \min\left(e_{i,j}^x, e_{i,j+1}^x\right) \qquad (9)$$

4. Adaptive cutter path planning

In this section, an algorithm of cutter path planning is proposed so that the machined surface error can be limited to tolerance and the machining can be performed with a considerable reduction of the machining time. The proposed methodology enables the IOM to choose different grids adaptively based on the surface slopes and curvatures rather than constant grid sizes. As the grid sizes are used adaptively based on geometric characteristic of the surface, the proposed path planning is called adaptive cutter path planning.

The machined surface error analysis is carried out for each bounded area in a rectangular grid of CL-points generated by the IOM with constant grid size. Then the rectangular grid of points is refined through the segmentation if the machined surface error exceeds tolerance. The segmentation in the forward direction is related to the number of linear segments required to complete the tool path and in practice, it is related to the size of CNC program rather than the total distance (or the machining time) of the cutter path [28]. Whereas segmenting in the transverse direction increases the total distance of the cutter path and, consequently, the machining time. Therefore, segmentation in the forward direction is preferred first and when it reaches to the minimal value limited by the controller then only the segmentation in the transverse direction is performed. Given a $(m \times n)$ grid of CL-points generated with constant grid sizes g^x (x-direction) and g^y (y-direction), the following segmentation strategy is adopted:

- Firstly, the chordal deviations and cusp heights are estimated using Eqs. (5) and (8) respectively and if their absolute values exceed a specified tolerance ε_a then there is a segmentation to reduce the error within tolerance. The segmentation is performed by choosing the grid sizes $\dfrac{g^x}{2}$, $\dfrac{g^x}{3}$, ..., $\dfrac{g^x}{M}$ (M is an integer) in the x direction and $\dfrac{g^y}{2}$, $\dfrac{g^y}{3}$, ..., $\dfrac{g^y}{N}$ (N is an integer) in the y direction respectively until the error becomes within ε_a. The purpose of the analysis is to predict the maximum value of M and N. The radii of curvature and slope angles are unchanged during segmentation.

- Subsequently, the combined effect of the cusp height and negative chordal deviation is estimated using Eq. (9) and if the value exceeds ε_a then there is a further segmentation to reduce the error within tolerance. Then the segmentations in the x-direction are carried out until the new chordal deviation $\left(\min\left(e_{i,j}^{\prime x}, e_{i,j+1}^{\prime x}\right)\right)$ is limited by the following expression:

$$\min\left(e_{i,j}^{\prime x}, e_{i,j+1}^{\prime x}\right) \geq \max\left(e_{i,j}^{y}, e_{i+1,j}^{y}\right) - \varepsilon_{a} \tag{10}$$

The segmentation in the forward direction is conducted according to Eq. (10) so that the machined surface error for every machining strip is always controlled within tolerance. In certain cases, the value of g^x may be zero in order to maintain the chordal deviation specified by Eq. (10). To overcome this situation, the lowest limit of the grid size δ, the minimum distance between two movements of a cutter for a CNC controller, is specified. If g^x reaches the value of δ then the segmentation in the transverse direction must be carried out. The new value of the chordal deviation $\left(\min\left(e_{i,j}^{\prime\prime x}, e_{i,j+1}^{\prime\prime x}\right)\right)$ is calculated using the value of $g^x = \delta$ and the segmentations of the path-interval g^y are carried out until the new cusp height $\left(\max\left(e_{i,j}^{\prime y}, e_{i+1,j}^{\prime y}\right)\right)$ is limited by the following expression:

$$\max\left(e_{i,j}^{\prime y}, e_{i+1,j}^{\prime y}\right) \leq \varepsilon_{a} + \min\left(e_{i,j}^{\prime\prime x}, e_{i,j+1}^{\prime\prime x}\right) \tag{11}$$

The adaptive grid is generated in the following steps:

Step 1

Compute the slope angles $\alpha_{i,j}^{x}$ and $\alpha_{i,j}^{y}$ for every CL-curve segment and the radii of curvature $\rho_{i,j}^{x}$ and $\rho_{i,j}^{y}$ at every CL-point $\mathbf{CL}_{i,j}$ where i = 0, 1, …, m and j = 0, 1, …, n generated using the constant grid sizes in the x and y directions .

Step 2

Check the machined surface error for the bounded area and segment until the machined surface error is less than ε_{a}. Find the number of segments $k_{i,j}^{x}$ and $l_{i,j}^{y}$ where i = 0, 1, …, m-1 and j = 0, 1, …, n-1 in the x and y directions respectively for all bounded areas.

Step 3

Once all number of segments have been determined for all bounded areas in both directions, determine the maximum number of segments r_{i}^{x} where i = 0, 1, …, m-1 and s_{j}^{y} where j = 0, 1, …, n-1 in the whole rectangular strip (from one end to other) in the x and y directions. Final number of segments in the x and y directions for adaptive grid generation are as follows:

$r_{i}^{x} = \max\{k_{i,0}^{x}, k_{i,1}^{x}, ..., k_{i,n-1}^{x}\}$ where i = 0, 1, …, m-1

$s_{j}^{y} = \max\{l_{0,j}^{y}, l_{1,j}^{y}, ..., l_{m-1,j}^{y}\}$ where j = 0, 1, …, n-1

Step 4

Generate adaptive 2D grid of points in the xy-plane using the number of segments r_{i}^{x} and s_{j}^{y} computed at *Step 3* in the x and y directions respectively.

Step 5

Generate the CL-points with the adaptive grids generated at *Step 4* and carry out the error analysis to check whether the machined surface error in every region is within tolerance. If the machined surface error exceeds tolerance then repeat the whole procedure.
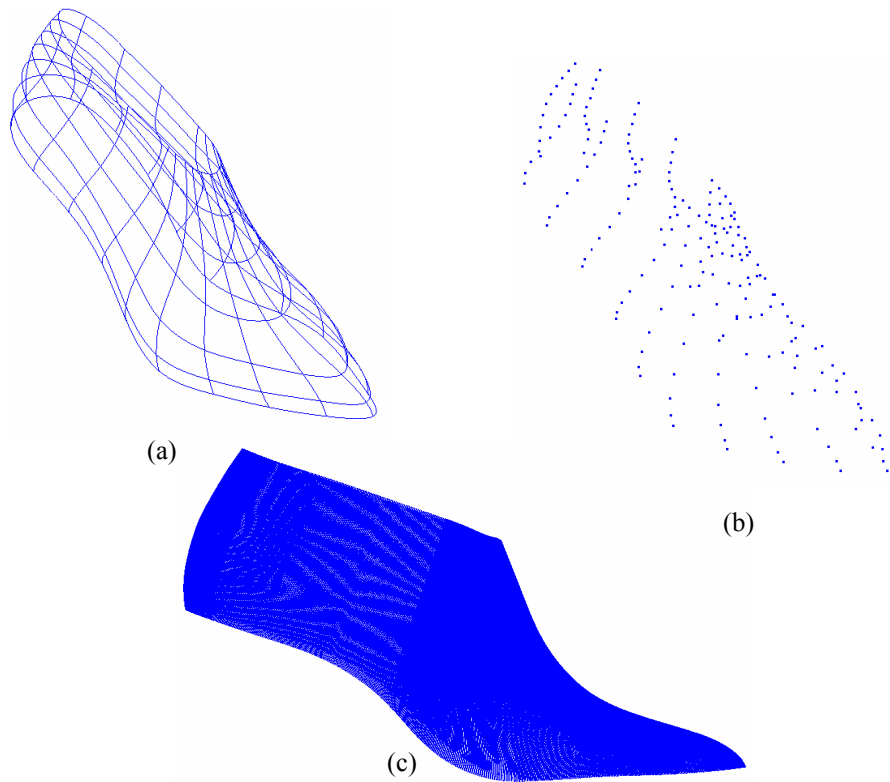
Fig. 5. Shoe-last model: (a) 120 bi-cubic Bézier surface model (b) Points characterizing model and (c) Set of points for machining

5. Machining example

The machining of the shoe last model is considered for the case study. The surface model consisting of 120 bi-cubic Bézier surfaces, as shown in figure 5(a), is characterised by a (10×21) grid of surface points (shown in figure 5(b)) that defines the surface shape within 1.0 mm tolerance. Assuming that a suitable interpolation scheme is available, the grids of discrete points used in the shoe-last model have been sampled from parametric surface definition but the algorithm is equally applicable to any grid of points with any interpolation scheme. A ball-end mill of 2.5 mm radius is used for machining. A (601×1381) grid of points (shown in figure 5(c)) that ensures that the offset surface can be generated with 0.01 mm tolerance [12], is used for generating cutter paths with constant grid sizes g^x = 0.5 mm and g^y = 0.5 mm, as shown in figure 6 where the total number of CL-points (321×541) is generated. The step-interval distance in the heel area with high slopes is larger than that the flatter area, as shown in figure 6, and therefore, the machined surface error in the heel area exceeds tolerance. In a 5.0 mm distance, as shown in figure 6, the chordal deviation and the cusp height for the cutter paths generated with constant grid sizes have been estimated for strips 1-10, as listed in Table 1.

Strip no.	Max. chordal deviation (mm)	Max. cusp height (mm)	Max. machined surface error (mm)	No. of segments
1	0.014	0.773	0.773	6
2	0.010	0.544	0.544	6
3	0.004	0.442	0.442	5
4	0.004	0.214	0.214	4
5	0.010	0.179	0.179	3
6	0.005	0.130	0.130	3
7	0.005	0.086	0.086	2
8	0.003	0.105	0.105	2
9	0.005	0.097	0.097	2
10	0.003	0.042	0.042	2

Table 1. Estimated machined surface error for strips 1-10

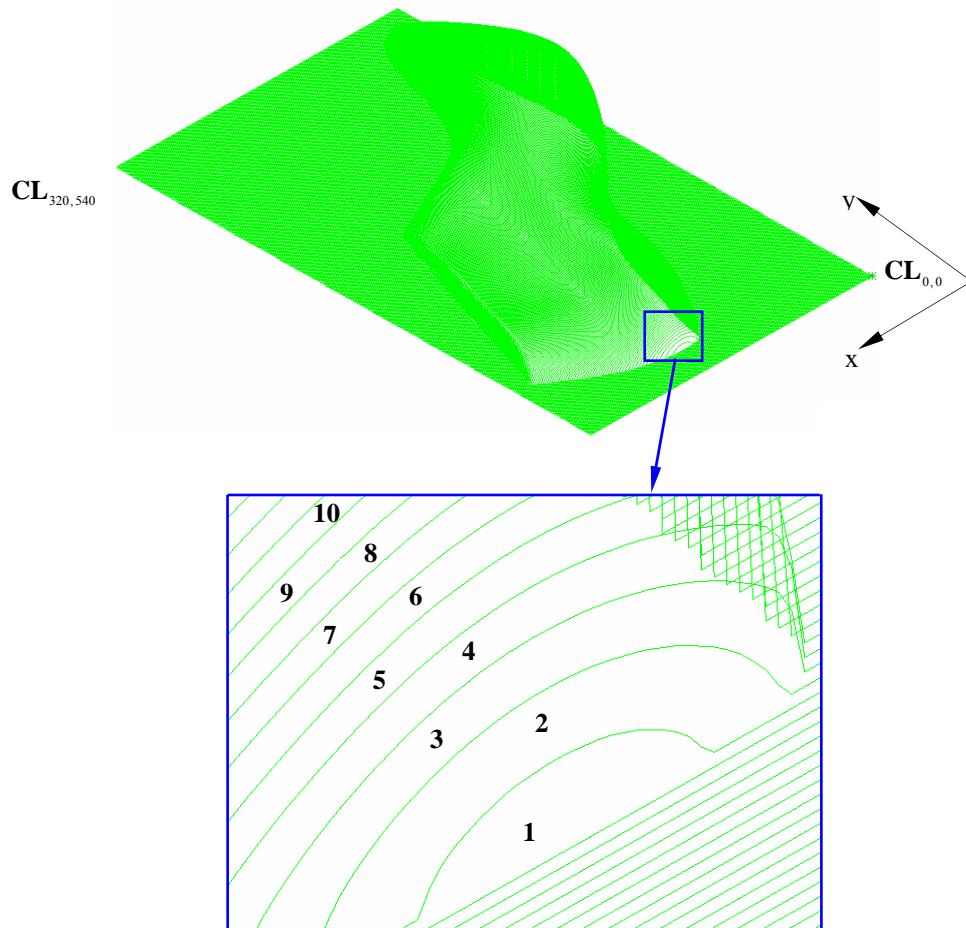**Fig. 6.** Cutter paths with constant grid sizes
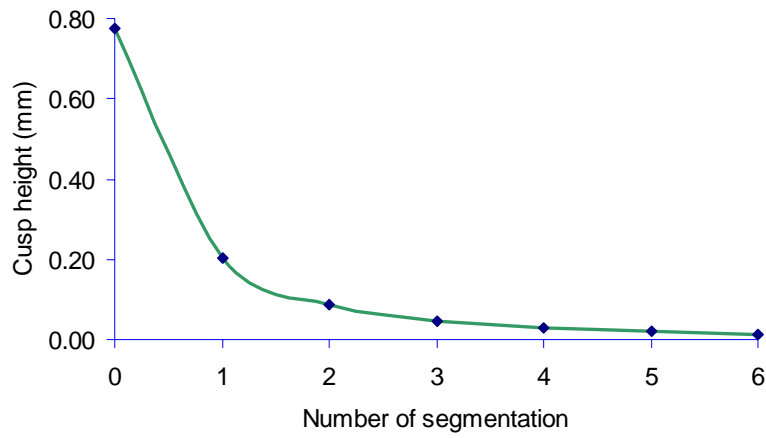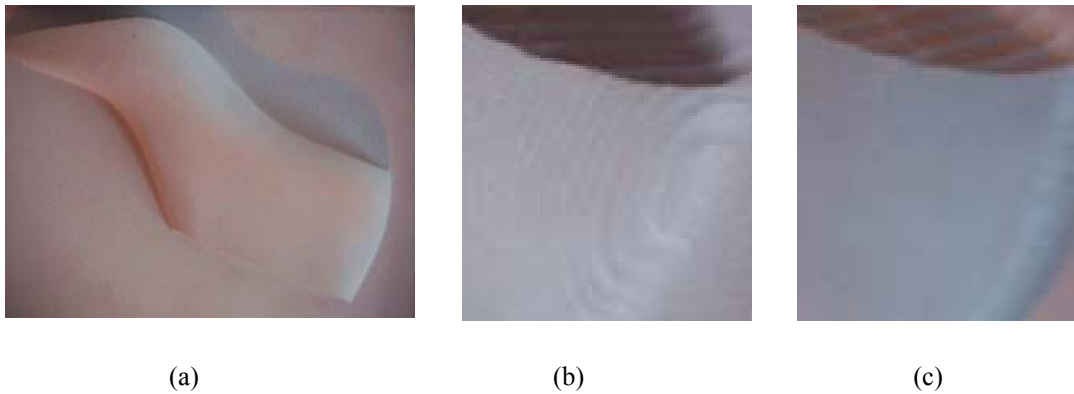
Fig. 7. Reduction of cusp height with number of segmentation

(a)   (b)   (c)

Fig. 8. Machined shoe: (a) Constant grid sizes based planning

(b) Enlarged view of machining flaw and (c) Adaptive cutter path planning

It is evident that the chordal deviation is within 0.01 mm (approximation with two decimal places) but the cusp height exceeds the allowable limit 0.01 mm. The resultant machined surface error for this bounded area is governed by the boundary segments due to the positive chordal deviations. Thus the segmentation is to be carried out in the transverse direction in order to limit the cusp height within 0.01 mm. The reduction of the cusp height for increasing the number of segmentation is illustrated in figure 7 for strip-1. It is evident that the cusp height reduces drastically after the first segmentation and it does not reduce much though number of segmentation increases and finally, the cusp height becomes within 0.01 mm after 6 segmentations for strip-1. For other strips 2-10, 6-2 segmentations are required for a 4.5 mm distance. As a result, the adaptation increases the grid sizes from 321×541 to 321×576 and a further adaptation with a further increase in the grid sizes would be needed to correct the machining in the toe region. The cutter paths are also generated from the adaptive grid sizes using the IOM and then the error

analysis is performed on these CL-points. It has been found that the machined surface errors are well within 0.01 mm for adaptive cutter paths. As the error estimation is dependent on the curvature value that is estimated from the point data using the circle based three-point and five-point formulas, the curvature estimation becomes more accurate for more number of point data [25] and hence, the resultant error in adaptive grids becomes well within allowable limit.

In order to assess the estimated machined surface error, the shoe last model is machined with constant grid sizes g^x = 0.5 mm and g^y = 0.5 mm in Hermle C600U 5-axis machining centre equipped with a Heidenhain TNC430 controller. The cutting parameters such as the cutting speed 1000 mm/min and spindle speed 3000 mm/min are used for finish machining. The resulting machined surface is shown in figure 8(a) with a detailed view of the heel area in figure 8(b) where the maximum cusp height is 0.773 mm due to highly sloped region in the transverse cutting direction. The adaptive grid generation method is applied in the heel area and the machining is performed with adaptive cutter paths. Figure 8(c) shows the local result with the adaptive cutter paths, which demonstrates that the proposed method of adaptive cutter path generation can effectively control the machined surface error within tolerance. In the uniform grid approach, the minimum grid sizes 0.5 mm and 0.08 mm respectively in forward and transverse directions are needed to limit the machined surface error within 0.01 mm. If these minimal grids are used uniformly for the entire surface, the estimated machining time becomes 671 minutes. On the other hand, the entire shoe is machined only in 220 minutes when the adaptive grids are applied. As a result, the machining efficiency is increased by 67.2% compared to the uniform minimal grid method.

6. Conclusions

In this paper, the chordal deviation and cusp height are derived with consideration to the surface slopes and curvatures in the forward and transverse directions respectively, and the machined surface error is estimated as a combination of the chordal deviation and cusp height. In contrast with the constant grid approach, an adaptive grid generation algorithm is proposed, which determines number of segmentations in respective directions in order to limit the machined surface error within tolerance. As a result, the inverse offset method generates cutter paths from the point-based surface adaptively using the different step-forward and step-interval distances in different regions so that the machined surface error is limited within tolerance and the machining is performed with considerable reduction of the machining time. However, it is recognised that the accuracy of the machined surface error estimation is dependent on the curvature value that is determined using the circle based three-point and five-point formulas in this paper. Therefore, a sophisticated curvature estimation method certainly increases the accuracy of the error estimation and consequently, the performance of the adaptive cutter path generation.

In the proposed approach, the adaptive grids are generated in such a way that the rectangular topology is maintained and as a result, there is much redundant CL data in the gentle sloped areas. In order to reduce the redundant CL-data, one approach is to decompose the point-based surface into different regions and generate cutter paths in each region independently and machine each region separately. Although the machining time is reduced in the region-by-region approach, the tool marks left at the boundary tend to be pronounced, which may adversely affect the surface quality in finish machining. Therefore, further research is needed to correct this disadvantage by connecting the cutter paths of the two neighbouring regions in order to obtain a smooth finished surface.

Acknowledgements

References

1. Park, S.C. (2004), Sculptured surface machining using triangular mesh slicing, *Computer-Aided Design*, 36, 279-288.

2. Lee, S.G., and Yang, Y.H. (2002), CNC tool-path planning for high speed high-resolution machining using a new tool-path calculation algorithm, *International Journal of Advanced Manufacturing Technology*, 20, 326-333.

3. Kim, S.J., and Yang, M.Y. (2006), A CL surface deformation approach for constant scallop height tool path generation from triangular mesh, *International Journal of Advanced Manufacturing Technology*, 28, 314-320.

4. Loney, G.C., and Ozsoy, T.M. (1987), NC machining of free-form surfaces, *Computer-Aided Design*, 19, 85-90.

5. Elber, G., and Cohen, G. (1994), Tool-path generation from free-form surface models, *Computer-Aided Design*, 26, 490-496.

6. Feng, H.Y., and Li, H. (2002), Constant scallop-height tool path generation for three-axis sculptured surface machining, *Computer-Aided Design*, 34, 647-654.

7. Choi, B.K., Chung, Y.C., Park, J.W., and Kim, D.H. (1994), Unified CAM-system architecture for die and mould manufacturing, *Computer-Aided Design*, 26, 235-243.

8. Park, S.C. (2003), Tool-path generation for Z-constant contour machining, *Computer-Aided Design*, 35, 27-36.

9. Ding, S., Mannan, M.A., Poo, A.N., Yang, D.C.H, and Han, Z. (2003), Adaptive iso-planar tool path generation for machining of free-form surfaces, *Computer-Aided Design*, 35, 141-153.

10. Lin, R.S., and Koren, Y. (1996), Efficient tool-path planning for machining free-form surfaces, *Transaction of the ASME- Journal of Engineering for industry*, 118, 20-28.

11. Suresh, K. and Yang, D.C.H. (1994), Constant scallop-height machining of free-form surfaces, *ASME Journal of Engineering for Industry*, 116, 253–259.

12. Yoon, J.-H. (2005), Fast tool path generation by iso-scallop height method for ball-end milling of sculptured surfaces, *International Journal of Production Research*, 43, 4989-4998.

13. Kayal, P. (2007), Offset error analysis of ball-end mill for cutter path generation from point-based surfaces, *International Journal of Advanced Manufacturing Technology*, (press)

14. Lin, A.C., and Liu, H.T. (1998), Automatic generation of NC cutter path from massive data points, *Computer-Aided Design*, 30, 77-90.

15. Park, S.C., and Chung, Y.C. (2003), Tool-path generation from measured data, *Computer-Aided Design*, 35, 467-476.

16. Kishinami, T., Kondo, T., and Satio, K. (1987), Inverse offset method for cutter path generation, *Proceedings of the 6th International Conference on Production Engineering*, Osaka, 807-812.

17. Kayal, P., and Ball, A.A. (2004), A point-based approach for free-form surface finishing and its quality assessment compared to polyhedral machining, *Proceedings of the International Symposium on Advanced Materials and Processing*, Indian Institute of Technology, Kharagpur, India, 358-365.

18. Takeuchi, Y., Sakamoto, M., Abe, Y., and Orita, R. (1998), Development of a personal CAD/CAM system for mold manufacture based on solid modelling techniques, *Ann. CIRP* 38, 429-432.

19. Inui, M. (2003), Fast inverse offset computation using polygon rendering hardware, *Computer-Aided Design*, 35, 191-201.

20. Choi, B.K., Kim, D.H. and Jerard, R.B. (1997), C-space approach to tool-path generation for die and mold machining, *Computer-Aided Design*, 29, 657-669.

21. Zhang, X., Wang, J., Yamazaki, K., and Mori, M. (2004), A surface based approach to recognition of geometric features for quality freeform surface machining, *Computer-Aided Design*, 36, 735-744.

22. Feng, H.Y. and Teng, Z. (2005), Iso-planar piecewise NC tool path generation from discrete measured data points, *Computer-Aided Design*, 37, 55-64.

23. PowerMILL Manual. (2002), *Delcam plc*, England.

24. Lee, E. (2003), Contour offset approach to spiral tool path generation with constant scallop height, *Computer-Aided Design*, 35, 511-518.

25. Chuang, C.M. and Yau, H.T. (2005), A new approach to z-level contour machining of triangulated

surface models using fillet endmills, *Computer-Aided Design*, 37, 1039-1051.

26. Tookey, R.M., and Ball, A.A. (1997), Estimation of curvatures from planar point data, *Mathematics of Surfaces VII*, *Information of Geometers*, 131-144.

27. Kayal, P., and Ball, A.A. (2005), Adaptive raster cutter path scheduling for free-form surface machining, *Proceedings of 2nd JSME/ASME International Conference on Materials and Processing*, Seattle, Washington, USA, MEP-07: 1-5.

28. Lo, C.H., and Lin, R.S. (2001), An improved method for scheduling the tool paths for three-axis surface machining, *International Journal of Machine Tools and Manufacture*, 41, 133-141.

Author's Biographies

Prasenjit Kayal is a member of Society of Manufacturing Engineers (SME), USA. He has a long term industrial research career in Engineers India Limited, India where he is involved in Engineering and Technology Development for above/under-ground piping, buried/offshore pipelines, pressure vessels and heat exchangers in petrochemical, refinery and gas processing industries. He has published several peer reviewed journal papers, and also presented papers in international conferences in India, USA and UK. His scientific interests include geometry-based algorithm for cutter path generation, 3-axis and 5-axis CNC machining, finite element analysis and stress analysis. This work was executed while he was doing research in School of Engineering (Mechanical), University of Birmingham, UK.